Deficiency of Voltage-gated Proton Channel Hv1 Leads to hypoinsulinaemia, hyperglycemia and glucose intolerance in mice

Xudong Wang[a,1], Qing Zhao[a,c,1], Wang Xi[a], Shangrong Zhang[a], Jiwei Qin[a], Jili Lv[a], Yongzhe Che[b], Weiyan Zuo[a], Shu Jie Li[a,b,c,#]

[a]Department of Biophysics, School of Physical Science, The Key Laboratory of Bioactive Materials, Ministry of Education, Nankai University, Tianjin 300071, P. R. China

[b]Department of Physiology, School of Medicine, Nankai University, Tianjin 300071, P. R. China

[c]Department of Cellular and Molecular Biology, School of Life Science, Tianjin 300071, P. R. China

Running title: Loss of Hv1 leads to hypoinsulinaemia

Address correspondence to: Dr. Shu Jie Li, Department of Biophysics, The Key Laboratory of Bioactive Materials, Ministry of Education, Nankai University, 94 Weijin Road, Nankai District, Tianjin 300071, P. R. China, Tel & Fax: +86-22-2350-6973, Email: shujieli@nankai.edu.cn

Keywords: Voltage-gated proton channel Hv1; Pancreatic islets; β cells; Insulin secretion; Hyperglycemia; Diabetes

SUMMARY

Here, we demonstrate that the voltage-gated proton channel Hv1 represents a regulatory mechanism for insulin secretion of pancreatic islet *β* cell and glucose homeostasis. *In vivo*, Hv1-deficient mice display hypoinsulinaemia, hyperglycemia and glucose intolerance due to reduced insulin secretion, but normal peripheral insulin sensitivity. *In vitro*, islets from Hv1-deficient and heterozygous mice, *β* cells and islets with siRNA-mediated knockdown of Hv1 exhibit a marked defect in secretagogue-induced insulin secretion. A decrease in *α* and *β* cell masses has been observed in islets from Hv1-deficient mice. Furthermore, Hv1-deficient *β* cell has an impairment on glucose- and sulfonylurea-induced intracellular Ca^{2+} homeostasis and membrane depolarization. Collectively, our *in vitro* and *in vivo* results indicate that Hv1 is required for insulin secretion in the *β* cell and that dysfunction of Hv1 may contribute to the pathophysiology of type 2 diabetes. Our study sheds light on a new biological function of the proton channel.

INTRODUCTION

Glucose homeostasis in mammals is tightly controlled, in large part, by pancreatic *β* cells, which secrete insulin in proportion to increasing concentrations of glucose. Insulin reduces blood glucose by stimulating use of glucose by peripheral tissues and inhibiting hepatic glucose production (Warram et al., 1994). Type 1 diabetes and type 2 diabetes are both characterized by uncontrolled hyperglycemia, and maintenance of blood glucose within a physiological range is critical for the prevention of diabetes-related complications (reviewed in Kahn, 2000). Type 1 diabetes is defined as hyperglycemia when insulin is extremely low or absent due to absolute deficiency of *β* cell mass. The pathogenesis of type 2 diabetes involves both insulin resistance in muscle, fat and liver, and decreased insulin secretion in pancreatic *β* cells (Defronzo, 2009; Martin et al., 1992; Olefsky and Glass, 2010; Weir and Bonner-Weir, 2004).

In the early prediabetic state, pancreatic islets respond to the increased insulin

secretion to generate compensatory hyperinsulinemia for the resistance to insulin and maintain relative euglycemia (DeFronzo et al., 1992). The subsequent development of hyperglycaemia results from the failure of β cells to secrete enough insulin for effective compensation (DeFronzo et al., 1992). This β cell dysfunction is largely manifested as impaired glucose-stimulated insulin secretion (GSIS) and can be detected in the earliest stages of type 2 diabetes with complete loss of first phase GSIS (Weir and Bonner-Weir, 2004). In fact, one of the characteristics of this defect is a failure of the β cell to respond to a glucose stimulus while retaining its response to other secretagogues such as amino acids (Porte, Jr., 1991). The regulation of insulin secretion from the β cell is complex, and the molecular defects underlying the relative failure of the β cell in type 2 diabetes are still unclear.

The voltage-gated proton channel Hv1 is involved in regulating intracellular pH during "respiratory burst", in which Hv1 compensates the cellular loss of electrons with protons required for NADPH oxidase (NOX)-dependent ROS generation (Decoursey, 2003, Ramsey et al., 2009). Clapham's group found that Hv1 contributes to brain damage in cerebral ischemia through regulating NOX-dependent ROS generation (Wu et al., 2012). Kirichok's group successfully recorded proton current of Hv1 in human spermatozoa by patch clamp, and demonstrated that Hv1 is dedicated to inducing intracellular alkalinization and activating spermatozoa (Lishko et al., 2010). Moreover, the recent studies showed that Hv1 plays important roles in breast (Wang et al., 2011; Wang et al., 2012) and colorectal (Wang et al., 2013a) cancer and glioma (Wang et al., 2013b) development, progression and metastasis, through regulating cancer cell intracellular pH and resulting in tumor acidic microenvironment.

In our previous study, we have identified that the voltage-gated proton channel Hv1 is present in human and rodent pancreatic islet β cells, as well as β cell lines (Zhao et al., 2015). In present study, we have discovered a regulatory pathway for the voltage-gated proton channel Hv1 in the modulation of β cell insulin secretory function. We found that Hv1 knockout (Hv1KO) mice develop hyperglycemia and a glucose intolerance with reduced insulin secretion. Deficiency of Hv1 inhibits insulin secretion in response to a

variety of stimuli from isolated islets, and has an impairment on glucose- and sulfonylurea-induced intracellular Ca^{2+} homeostasis and membrane depolarization in the β cell. Our results suggest that Hv1 deficiency may contribute to type 2 diabetes.

EXPERIMENTAL PROCEDURES

Animals and treatments

Mice bearing a targeted disruption in the VSOP/Hv1 (VSOP/Hv1$^{-/-}$, backcrossed eight times) were kindly provided by Dr. Y. Okamura (School of Medicine, Osaka University), as previously described (Okochi et al., 2009). WT mice (VSOP/Hv1$^{+/+}$) were of the same genetic background (C57BL/6J). Animals were kept in a pathogen-free facility under a 12-h light-dark cycle with access to water and a standard mouse diet (Lillico Biotechnology). Genotyping was performed by PCR as described by Ramsey et al. (Ramsey et al., 2009). Experiments were performed with 2 and 4 month-old male mice, unless indicated otherwise. All animal husbandry and experiments were approved by and performed in accordance with guidelines from the Animal Research Committee of Nankai University.

Blood glucose and insulin determinations

Blood glucose levels were measured from blood obtained from the tail vein after Fasting 6 h using an automated glucometer (One Touch, Johnson & Johnson, USA). For glucose tolerance tests, mice at 2 and 4 months of age were fasted for 6 h before intraperitoneal (i.p.) injection with glucose (2 g/kg body weight), and blood glucose concentration was measured at 0, 15, 30, 60 and 120 min after the injection. For insulin tolerance tests, mice were fasted for 6 h before intraperitoneal injection with insulin (1.0 units/kg body weight), and blood glucose concentration was measured at 0, 15, 30, 60 and 120 min.

For serum insulin measurements, glucose (2 g/kg body weight) or L-arginine (1 g/kg body weight) was injected i.p., and venous blood was collected at 0, 2, 5, 15, and 30 min in chilled heparinized tubes, immediately centrifuged, and the serum stored at -80^{o}C. Insulin levels were measured by ELISA (Mercodia, Uppsala).

Isolation of pancreatic islets

Pancreatic islets were isolated according to the collagenase digestion method described by Lacy and Kostianovsky (Lacy and Kostianovsky, 1967), with slight modifications. Krebs-Ringer bicarbonate HEPES (KRBH) buffer (in mM: 135 NaCl, 3.6 KCl, 5 $NaHCO_3$, 0.5 NaH_2PO_4, 0.5 $MgCl_2$, 1.5 $CaCl_2$, 10 HEPES, pH 7.4) was used for islet isolation. And the isolated islets were cultured overnight in RPMI 1640 (GIBCO) containing 10% fetal bovine serum (FBS) in a humidified 5% CO_2 atmosphere at 37^{o}C before handpicking for experiments as previously described (Zhao et al., 2015).

Cell culture

Pancreatic islet β cell line, INS-1 (832/13) cells were obtained from Dr. Hans Hohmeier (Duke University) and grown in RPMI 1640 medium (GIBCO) supplemented with 10% FBS, 2 mM glutamate, 1 mM sodium pyruvate and 55 μM β-mercaptoethanol in a humidified 5% CO_2 atmosphere at 37^{o}C.

siRNA silencing

To down-regulate Hv1 expression level in isolated islets and β-cells, the sequences of the small interfering RNA (siRNA) targeting the Hv1 gene 5'-CTACAAGAAATGGGAGAAT-3' and the scramble sense sequence 5'-TTCTCCGAACGTGTCACGT-3', which were obtained from Ribobio (Guangzhou, China), were used, as described previously (Zhao et al., 2015).

Quantitative real-time PCR

The mRNA expression levels of insulin in isolated islets and INS-1 (832/13) β cells, were evaluated by quantitative real-time PCR using ABI PRISM 7000 Sequence Detection System (Applied Biosystems, Foster City, CA), as described previously (Zhao et al., 2015). The primers were as follows: insulin, 5'- CCTCACCTGGTGGAGGCTC-3' (forward) and 5'-ACAATGCCACGCTTCTGC-3' (reverse); GAPDH, 5'-CCAAGGTCATCCATGACAAC-3' (forward) and 5'-AGAGGCAGGGATGATGTTCT-3' (reverse). All experiments were performed in triplicate.

Insulin secretion assay

Insulin secretion from isolated islets and INS-1 (832/13) β cells was measured as previously described (Zhao et al., 2015). Total insulin and proinsulin content in isolated islets and INS-1 (832/13) cells were extracted with acidic ethanol and determined using rat/mouse proinsulin, mouse and rat insulin ELISA (Mercodia, Uppsala), according to the manufacturer's protocol.

Serum glucagon determinations

To test the effect of Hv1 on glucagon secretion, mice were fasted for 6 h before intraperitoneal injection with insulin (1.0 units/kg body weight). And serum glucagon levels during insulin tolerance tests (ITT) were determined at 0, 20 and 40 min using glucagon ELISA (Mercodia, Uppsala), according to the manufacturer's protocol.

Immunohistochemistry

Immunohistochemistry was performed as described previously (Zhao et al., 2015).

Immunnofluorescence

Immunofluorescence was performed as described previously (Zhao et al., 2015).

Islet cAMP content

Islets in groups of 50 were preincubated for 1 h at 2.8 mM glucose in KRBH/BSA, and then stimulated with 16.7 mM glucose in the presence of 10 μM forskolin for 30 min at 37°C. After the supernatants were removed, the islets were washed once with ice-cold KRBH, and then ice-cold HCl (100 μl, 0.1 mM) was added to islet pellets followed by 10 min agitation at 4°C. After neutralization with 100 μl 0.1 mM NaOH, islet cAMP contents were determined using an Enzyme Immunoassay kit (Sigma-Aldrich, St Louis, MO) according to the manufacturer's protocol.

Measurements of intracellular Ca^{2+}

Cellular Ca^{2+} changes were monitored as previously described (Zhao et al., 2015).

Measurements of membrane potential

The voltage-sensitive bis-oxonol fluorescent dye $DiBAC_4(3)$ was used to study the membrane potential changes of INS-1 (832/13) β cells. The β cells transfected with the scramble or Hv1-targeting siRNA were incubated with 2 μM $DiBAC_4(3)$ for 10 min at 37°C in a solution (in mM: 138 NaCl, 5.6 KCl, 1.2 $MgCl_2$, 2.6 $CaCl_2$, 2.8 glucose and 10

HEPES, pH 7.4) prior to fluorescence measurement. Data were expressed as an average of five experiments (50-80 cells per experiment).

Statistical analysis

All statistics were performed using SPSS20.0 software. Measurement data were represented as mean ± SEM. Comparison of the mean between groups was performed by *t* test. *P* values < 0.05 were considered significant.

RESULTS

Hv1-deficient mice exhibit hyperglycaemia and impaired glucose tolerance due to reduced insulin secretion

To assess the effect of Hv1 knockout on glucose homeostasis, glucose levels were measured in 4 month-old mice in fasted state. The body weight curves of the control (WT, $Hv1^{+/+}$), heterozygous ($Hv1^{+/-}$) and homozygous (KO, $Hv1^{-/-}$) littermates were almost similar (Fig. 1A), but the blood glucose levels in fasted state were markedly higher in heterozygous (9.3 ± 0.4 mmol/l, n = 24, $p < 0.001$) and KO (10.2 ± 0.6 mmol/l, n = 24, $p < 0.001$) mice compared with WT mice (6.2 ± 0.2 mmol/l, n = 24) (Fig. 1B).

To evaluate the impact of Hv1 on disposal of a glucose load, intraperitoneal (i.p.) glucose tolerance tests (IPGTT) were performed. Compared with WT mice, both KO and heterozygous mice in 2 and 4 months of age showed significantly higher glucose levels following an i.p. glucose load (2 g/kg body weight) (Fig. 1C and Fig. 2A). Corresponding serum insulin levels (including basal) were lower in both KO and heterozygous mice throughout the IPGTT after the glucose challenge compared with WT mice, providing evidence for an insulin secretion defect in response to glucose (Fig. 1D and Fig. 2B). Interestingly, KO and heterozygous mice exhibited a selective loss of acute first-phase insulin secretion in response to glucose (Fig. 1D and Fig. 2B). The insulin levels, however, did a little gradually rise after the glucose challenge, suggesting some retention of second-phase insulin secretion in both KO and heterozygous mice (Fig. 1D). Thus, the Hv1KO mice exhibit an impairment in their ability to dispose of a glucose load due to

insulin secretion defect.

To further evaluate the effect of Hv1 deletion on insulin secretion *in vivo*, insulin secretion in response to stimulation with arginine the major nutrient secretagogue of insulin was measured. The mechanisms of arginine-stimulated insulin secretion is independent on those by glucose, although the final pathways of secretion are the same (Weinhaus et al., 1997). Therefore, to determine the level of defect in glucose-stimulated insulin secretion, mice were also given an arginine challenge. As shown in Fig. 1E and Fig. 2C, serum insulin levels (including basal) were significantly lower in KO mice after the arginine injection (1 g/kg body weight) compared with WT mice. In contrast to the response to glucose, in both KO and heterozygous mice in 2 and 4 months of age, there was a first-phase insulin release in response to arginine (Fig. 1E and Fig. 2C).

To explore the possibility that the observed glucose intolerance was the result of peripheral insulin resistance, we performed i.p. insulin tolerance tests (IPITT) in Hv1KO mice in 2 and 4 months of age. We found that insulin administration lowered blood glucose levels in both WT and Hv1-deficient mice to a similar extent, indicating that Hv1 deficiency does not impair a peripheral insulin sensitivity (Fig. 1F and Fig. 2D). Taken Together, these data are compatible with the notion that loss of Hv1 results in impaired glucose tolerance due to a defect of insulin secretion *in vivo*.

Reduced insulin secretion of islets from Hv1-deficient mice

A mass of factors, however, can affect insulin secretion in vivo. To further delineate the role of Hv1 in insulin secretion, we performed insulin secretion assays using isolated islets from Hv1-deficient mice. As shown in Fig. 3A, 16.7 mM glucose-induced insulin secretion was greatly reduced by 51 (n = 8, $p < 0.001$) and 78% (n = 8, $p < 0.001$) in heterozygous and Hv1KO islets compared with WT islets (n = 8). While, basal insulin secretion (at 2.8 mM glucose) in heterozygous and KO islets was also significantly reduced by 60 (n = 8, $p < 0.001$) and 80% (n = 8, $p < 0.001$) compared with WT islets (n = 8). Similar results were observed for tolbutamide- and glibenclamide-induced insulin secretion in heterozygous and KO islets, which were significantly reduced by 78 (n = 8, $p < 0.001$)

and 85% (n = 8, $p < 0.001$), 61 (n = 8, $p < 0.001$) and 67% (n = 8, $p < 0.001$), for heterozygous and KO islets, respectively, compared with WT islets (n = 8) (Fig. 3A). Direct depolarization elicited by an increase of extracellular K^+ (60 mM KCl) also attenuated insulin secretion by 59 (n = 8, $p < 0.001$) and 65% (n = 8, $p < 0.001$) in heterozygous and KO islets compared with WT islets (n = 8) (Fig. 3A), indicating that knockout of Hv1 prevents K^+-induced insulin secretion in pancreatic β cells. Furthermore, arginine-induced insulin secretion of islets from heterozygous and KO mice was decreased by 67 (n = 8, $p < 0.001$) and 89% (n = 8, $p < 0.001$) compared with WT islets (n = 8) (Fig. 3A), as seen *in vivo*. Together, these data indicate that loss of Hv1 in islets inhibits insulin secretion.

Insulin and proinsulin contents in KO islets were reduced by 17 (n = 8, $p < 0.001$) and 25% (n = 8, $p < 0.01$), respectively, compared with WT islets (n = 8) at a basal condition (2.8 mM glucose) (Fig. 3B and C). The ratio of insulin to proinsulin content, however, was indistinguishable between KO and WT islets (Fig. 3D), suggesting that insulin synthesis is abnormal, but not insulin maturation in Hv1-deficient islets. The proinsulin secretion was barely detectable under basal conditions (2.8 mM glucose) in WT, heterozygous and KO islets (data not shown). In the presence of 16.7 mM glucose, the proinsulin secretion was reduced by 59 (n = 8, $p < 0.001$) and 78% (n = 8, $p < 0.001$) in heterozygous and KO islets, compared with WT islets (n = 8) (Fig. 3E). However, the ratios of insulin to proinsulin secretion in heterozygous and KO islets in the presence of 16.7 mM glucose were not different with WT islets (Fig. 3F), suggesting that no significant accumulation of proinsulin occurred in KO islets.

Knockdown of Hv1 inhibits secretagogue-induced insulin secretion

To further examine the effect of Hv1 on insulin secretion, we used RNA interference to instantaneously reduce endogenous Hv1 levels in INS-1 (832/13) β cells and isolated islets. The insulin secretion of the β cells and the islets at a basal condition (2.8 mM glucose) was low at both the controls and Hv1-knockdown β cells and islets (Fig. 4A and Fig. S1). In the presence of 16.7 mM glucose, 200 μM tolbutamide and 1 μM glibenclamide, the insulin secretion in the control β cells increased 9.6, 10.3 and 8.2-fold compared with

that at the basal condition, respectively. Whereas the insulin secretion was significantly reduced by 64 ($p < 0.001$), 60 ($p < 0.001$) and 73% ($p < 0.001$) by a reduction in Hv1 level with Hv1-targeting siRNA, respectively (Fig. 4A), indicating that Hv1 markedly affects the glucose- and sulfonylurea-induced insulin secretion in the β cells. In accordance with the β cells, the insulin secretion was reduced by 57 ($p < 0.001$), 48 ($p < 0.001$) and 57% ($p < 0.001$) in the Hv1-downregulated isolated islets compared with the controls at 16.7 mM glucose, 200 μM tolbutamide and 1 μM glibenclamide, respectively (Fig. S1).

To examine the effect of Hv1 on insulin processing, the insulin and proinsulin contents were measured. At a basal condition (2.8 mM glucose), the contents of both insulin and proinsulin were reduced by 36 ($p < 0.001$) and 39% ($p < 0.001$) respectively, in the Hv1-silenced β cells, compared with the controls (Fig. 4B and C). In comparison to the β cells, the contents of insulin and proinsulin were decreased by 42 ($p < 0.001$) and 40% ($p < 0.001$), respectively, in the Hv1-downregulated islets (Fig. S2A and B). However, the ratio of insulin to proinsulin content has a no difference between the controls and the Hv1-downregulated β cells (Fig. 4D) and islets (Fig. S2C), demonstrating that Hv1 has an impact on proinsulin synthesis. To further verify the effect of Hv1 on insulin synthesis, the insulin mRNA expression levels in the β cells and the isolated islets were measured. As shown in Fig 4E and F, insulin mRNA level was decreased by 38 ($p < 0.01$) and 33% ($p < 0.01$) by a reduction in Hv1 level with Hv1-targeting siRNA in the β cells and islets, respectively, compared with the controls, indicating that knockdown of Hv1 has an effect on insulin synthesis.

To detect the effect of Hv1 on proinsulin secretion, we then measured the proinsulin secretion in the β cells and isolated islets. The proinsulin secretion was barely detectable under basal conditions in both control and Hv1-silenced islets, but in the presence of 16.7 mM glucose, the proinsulin secretion was reduced by 68 ($p < 0.01$) and 63% ($p < 0.001$) by a reduction in Hv1 level, compared with the controls, in the β cells and islets, respectively (Fig. 4G and Fig. S3A). However, the ratio of insulin to proinsulin secretion in Hv1-silenced β cells and islets in the presence of 16.7 mM glucose was not different with that in control β cells and islets (Fig. 4H and Fig. S3B), suggesting that no significant

accumulation of proinsulin occurred in the Hv1-silenced β cells and islets.

Deficiency of Hv1 reduces α and β cell masses and pancreatic insulin content

The above results together showed that deletion of Hv1 inhibits insulin secretion *in vivo* and *in vitro*. To determine whether this may be due to the effect of Hv1 deletion on islet development, islet morphology, α and β cell mass, and pancreatic insulin content were measured. Morphometric analysis of pancreatic sections from WT, heterozygous and KO mice at 4 months of age exhibited a relatively normal islet architecture in each case, with β cells concentrated in the core and α cells located mainly in the periphery (Fig. 5A), while the morphology of isolated islets cultured overnight from KO mice is not overtly different from WT islets (data not shown). On the other hand, the number of the isolated islets per pancreas is not significantly different between WT and KO mice (data not shown) , which is consistent with the result from immunohistochemical analysis (Fig. S4A). However, the islet average size calculated from isolated islets (Fig. S4B) and islet area to total pancreas area (Fig. 5B) analyzed by immunohistochemistry of pancreatic sections were decreased in the KO mice compared with WT and heterozygous mice.

Interestingly, quantification of total α and β cell masses displayed a genotype-dependent difference. α and β cell masses were decreased by 71 (n = 6, $p < 0.01$) and 13% (n = 6, $p < 0.05$) in Hv1KO mice compared with WT mice (n = 6), respectively, as measured by morphometric analyses of insulin and glucagon positive islet cells (Fig. 5C and D). The total pancreatic insulin content in Hv1KO mice was also decreased by 11% (n = 6, $p < 0.05$) (Fig. 5E), the same as the observed in the isolated islets (Fig. 3B). These results show that Hv1KO mice have sufficient β cells and insulin, indicating that the *in vivo* phenotype is not due to a gross developmental defects.

Knockdown of Hv1 has no effect on cAMP generation

cAMP is an important second messenger involved in potentiating rather than initiating insulin secretion (Prentki et al., 1987). To detect the effect of Hv1 on cAMP production, we measured forskolin enhanced insulin secretion and cAMP content in isolated islets. In the

present of 10 μM forskolin, at 2.8 mM glucose, the insulin secretion in Hv1-silenced islets was decreased by 37% ($p < 0.01$) compared with that in control islets, while at 16.7 mM glucose, the insulin secretion was reduced by 63% ($p < 0.001$) (Fig. 6A). The cAMP content in Hv1-silenced islets was not different with that in control islets in the present of 10 μM forskolin and 16.7 mM glucose (Fig. 6B), suggesting that knockdown of Hv1 has no effect on cAMP production.

Glucagon-like peptide-1 (GLP-1) is an intestinally derived insulinotropic hormone, which increases cAMP generation and results in insulin release (Gromada et al., 2004). To further confirm the effect of Hv1 on cAMP production, we examined GLP-1-stimulated insulin secretion in Hv1-silenced INS-1 (832/13) β cells. At 16.7 mM glucose, 10 and 100 nM GLP-1 stimulated insulin secretion 2.3 and 2.7-fold over without GLP-1 (16.7 mM glucose) (Fig. 6C). However, the insulin secretion from the Hv1-silenced β cells was decreased by 73 ($p < 0.001$) and 53% ($p < 0.001$) in the presences of 10 and 100 nM GLP-1, respectively, compared with the control (Fig. 6C), indicating that the effect of Hv1 on insulin secretion is independent on cAMP pathway.

Deficiency of Hv1 impairs cellular Ca^{2+} homeostasis and membrane depolarization

Glucose stimulates insulin secretion by induction of Ca^{2+}-dependent electrical activity that triggers exocytosis of the insulin granules. We found that siRNA-mediated knockdown of Hv1 in INS-1 (832/13) β cells impaired tolbutamide-induced intracellular Ca^{2+} homeostasis (Fig. 6D and E). Zn^{2+} is a classical inhibitor of Hv1 (Ramsey et al., 2006; DeCoursey, 2008). 10 μM Zn^{2+} can efficiently inhibit Ca^{2+} influx stimulated by 200 μM tolbutamide (Fig. 6F). In pancreatic β cells, the increase of cytosolic Ca^{2+} ($[Ca^{2+}]c$) occurs with Ca^{2+} entry across voltage-sensitive Ca^{2+} channels activated by membrane depolarization (Rorsman and Renstrom, 2003). To confirm whether the abrogation of Ca^{2+} influx by suppression of Hv1 is coupled to membrane polarization, the membrane potential changes of INS-1 (832/13) β cells during glucose- and tolbutamide-stimulation were monitored with $DiBAC_4(3)$ fluorescence. As shown in Fig. 6G and H, the control cells were depolarized significantly more than Hv1-silenced INS-1 (832/13) β cells after glucose or

tolbutamide stimulation, indicating that Hv1 deficiency impairs glucose or tolbutamide-induced membrane depolarization. Thus, the reduction in insulin secretion by deficiency of Hv1 must therefore involve in electrical activity and $[Ca^{2+}]c$ signaling.

DISCUSSION

Here, we show *in vivo*, that both Hv1KO and heterozygous mice display hyperglycemia and glucose intolerance due to markedly decreased insulin secretion. Mice lacking the Hv1 show a loss of first-phase insulin secretion in response to glucose at both 2 and 4 months of age, but not to arginine, similar to that observed in humans with type 2 diabetes. *In vitro,* isolated islets and INS-1 (832/13) β cells with siRNA-mediated downregulation of Hv1, as well as islets isolated from both Hv1KO and heterozygous mice, exhibit significantly reduced secretagogue-induced insulin secretion. Interestingly, a decrease in α and β cell masses in Hv1KO mice has been observed, especially α cell mass. Taken together, these data indicate that the level of Hv1 expression in the β cell is critical for insulin secretion and maintaining glucose homeostasis, and reveal a significant role for the proton channel in the modulation of pancreatic α and β cell function.

The etiology of type 2 diabetes involves in insulin resistance and decreased β cell insulin secretion in order to develop the hyperglycemic diabetic state (Olefsky and Glass, 2010; Weir and Bonner-Weir, 2004). One of the features of this disease is a failure of the β cell to respond to a glucose stimulus while retaining its response to other secretagogues such as amino acids (Porte, 1991). A loss of first-phase insulin secretion in response to glucose has been observed in individuals destined to develop type 2 diabetes and can lead to hyperglycemia, which is thought to play an important role in the development of type 2 diabetes (Poitout and Robertson, 1996; Nesher et al., 1987; Temple et al., 1989). Studies in some animal models of diabetes found the loss of the acute phase secretion when reducing Glut2 levels in the β cell (Unger, 1991). This β cell dysfunction is largely manifested as impaired glucose-stimulated insulin secretion (GSIS) and can be detected in the earliest stages of type 2 diabetes with complete loss of first phase GSIS (Defronzo, 2009; Weir and Bonner-Weir, 2004). In fact, this failure has been detected in the individuals with maturity

onset diabetes of the young (MODY) who have genetic defects in transcription factors for β cell development and function or glucokinase, a key enzyme involved in glucorecognition in the β cell (Fajans, 1989; Froguel et al., 1992; Polonsky, 1995). However, the potential defect resulting in the selective loss of glucose response is not known.

The Hv1KO mice show a complete loss of glucose-stimulated first-phase insulin secretion and an inability to dispose a glucose challenge. In present study, we examined the insulin secretion pattern in Hv1KO mice using L-arginine that usually used to assess the first-phase insulin secretion in type 2 diabetes (Pfeifer et al., 1982). In striking contrast, the Hv1KO mice keep an arginine-stimulated first-phase insulin secretion, but the amount of first-phase is markedly reduced compared to those of the control animals. This is similar to humans with type 2 diabetes in which there is a loss of acute phase insulin secretion in response to glucose while maintaining the response to arginine (Pfeifer et al., 1982).

β cell failure in type 2 diabetes is associated with not only decreased β cell insulin secretory function but also reduced overall β cell mass (Weir and Bonner-Weir, 2004). In the prediabetic, islets enhance insulin secretion and β cell mass to generate compensatory hyperinsulinemia and maintain relative euglycemia duo to insulin resistance. However, when type 2 diabetes occurs, β cell secretory function and mass are significantly decreased and unable to compensate for the insulin resistance, resulting in the chronic hyperglycemic diabetic state. On the other hand, decreased β cell mass is usually not present at the time of diagnosis of type 2 diabetes (Rahier et al., 2008), suggesting that loss of β cell mass is not responsible for the onset of type 2 diabetes but rather is a consequence of diabetes.

In present study, total α and β cell masses display significant genotype-dependent differences. There was no difference in islet morphology between Hv1KO and WT mice, and only a very modest decrease in islet size and β cell mass, but a significant decrease in α cell mass. The smaller size observed in Hv1-deficient pancreatic islets may be related to the decrease in α and β cell masses, and may result from both impaired insulin and glucagon secretory function. In this context, it is important to note that *in vitro* siRNA-mediated knockdown of Hv1 in isolated islets and INS-1 (832/13) β cells caused decreased GSIS, suggesting that the *in vivo* decrease in insulin secretion in the Hv1KO mice was not due to

an *in vivo* β cell developmental defect.

Insulin secretion by pancreatic β cell is precisely regulated by glucose homeostasis (Warram et al., 1994). Glucose-induced insulin secretion has been proposed via two hierarchical signaling pathways (Henquin et al., 2003). Glucose metabolism generates ATP and results in the closure of ATP-sensitive K^+ channels and, as a consequence, the depolarization of the plasma membrane (Aguilar-Bryan and Bryan, 1999). This leads to Ca^{2+} influx through voltage-dependent L-type Ca^{2+} channels and a rise in cytosolic Ca^{2+} ($[Ca^{2+}]c$) which triggers insulin exocytosis (Rorsman and Renstrom, 2003; Barg, 2001). cAMP is an important intracellular massager for potentiation of glucose-stimulated insulin secretion (Seino et al., 2009; McQuaid et al., 2006). cAMP action in insulin secretion is well known to be mediated via the conversion of ATP to cAMP (Prentki and Matschinsky, 1987; Seino et al., 2009;) de Rooij et al., 1998). In present work, knockdown of Hv1 has no effect on cAMP production, suggesting that Hv1 does not influence the ATP generation.

Sulfonylureas such as tolbutamide and glibenclamide, bind to the SUR subunit of the ATP-sensitive K^+ channels and induce channel closure (Proks et al., 2002). We demonstrate that the lack of Hv1 inhibits sulfonylurea-induced insulin secretion, indicating that the effect of Hv1 on insulin secretion is not related to the ATP-sensitive K^+ channel pathway. We also show that ablation of the Hv1 gene abolishes the entry of calcium ions into the β cell evoked by glucose or tolbutamide. This important defect could be predicted from the reduced depolarization that we observed in the β cell. This indicates that β cells lacking Hv1 proton channel cannot generate Ca^{2+} influx when membrane cannot be depolarized. The fact that heterozygous mice also have a hyperglycemia with a low insulin level illustrates that Hv1 is at an important control point in the metabolic pathway regulating insulin secretion, and that relatively small changes in Hv1 activity are likely to have important effects on insulin secretion. Similar effects have been observed for glucokinase (Matschinsky et al., 1998). The findings of the present study clearly demonstrate that Hv1 plays an important role in positively regulating secretagogue-stimulated insulin secretion.

Taken together, the data in the present study demonstrate that Hv1-deficient mice

exhibit a hyperglycemia and impaired glucose tolerance with a completely loss of the acute phase insulin secretion in response to glucose, but normal peripheral insulin sensitivity. In striking contrast, a mouse with a deletion of Hv1 shows a attenuated first-phase insulin secretion in response to arginine. These findings provide direct evidence of a functional role for the proton channel in the maintenance of glucose homeostasis and might suggest that the insulin resistance may be not a sufficient factor in the development of a loss of glucose-stimulated insulin secretion. These studies also describe a novel pathway regulating β cell secretory function in which Hv1 sustains the entry of calcium ions into β cell through regulating membrane depolarization to promote increased insulin secretory responses. Considering that Hv1 is a positive regulator of insulin secretion and that relatively small changes in Hv1 levels significantly impact on insulin secretion, we hypothesized that decreased Hv1 expression might be associated with type 2 diabetes.

Acknowledgements

We would like to thank Dr. Y. Okamura (School of Medicine, Osaka University) for providing VSOP/Hv1 KO mice. We would like to thank Dr. Hans E. Hohmeier (Duke University Medical Center) for providing materials mentioned in the text. This work was supported by National Natural Science Foundation of China (No. 30970579 and 31271464), the Ph.D. Programs Foundation of Ministry of Education of China (No. 20110031110004 and 20120031110028), and the Basic Science and Advance Technology Research Program of Tianjin (No. 14JCYBJC23400).

Conflict of interest

The authors declare that they have no conflict of interest.

Author contributions

SJL, XDW and QZ conceived and designed the study. XDW, QZ, SRZ, WX, JWQ, YZC, JL, WYZ, DQL, YTG and SJL performed the experiments. SJL, XDW and QZ wrote the paper. SJL, XDW and ZQ reviewed and edited the manuscript. All authors were involved in data analysis, read and approved the manuscript.

REFERENCES

Aguilar-Bryan, L., and Bryan, J. (1999). Molecular biology of adenosine triphosphate-sensitive potassium channels. Endocr. Rev. *20*, 101-135.

Barg, B., Ma, X., Eliasson, L., Galvanovskis, J., Göpel, S.O., Obermüller, S., Platzer, J., Renström, E., Trus, M., Atlas, D., Striessnig, J., and Rorsman, P. (2001). Fast exocytosis with few Ca^{2+} channels in insulin-secreting mouse pancreatic B cells. Biophys. J. *81*, 3308-3323.

Decoursey, T.E. (2003). Voltage-gated proton channels and other proton transfer pathways. Physiol. Rev. *83*, 475-579.

DeCoursey, T.E. Voltage-gated proton channels: what's next? J. Physiol. *586*, 5305-5324 (2008).

DeFronzo, R.A., Bonadonna, R.C. and Ferrannini, E. (1992). Pathogenesis of NIDDM: a balanced overview. Diabetes Care *15*, 318-368.

Defronzo, R.A. (2009). Banting Lecture. From the triumvirate to the ominous octet: a new paradigm for the treatment of type 2 diabetes mellitus. Diabetes *58*, 773-795.

de Rooij, J., Zwartkruis, F.J., Verheijen, M.H., Cool, R.H., Nijman, S.M., Wittinghofer, A., and Bos, J.L. (1998). Epac is a Rap1 guanine-nucleotide-exchange factor directly activated by cyclic AMP. Nature *396*, 474-477.

Fajans, S.S. (1989). Maturity-onset diabetes of the young (MODY). Diab. Metab. Rev. *5*, 579-606.

Froguel, P, Vaxillaire, M, Sun, F, Velho, G, Zouali, H, Butal, M.O, Lesage, S, Vionnet, N, Clement, K, Fougerousse, F et al. (1992). Close linkage of glucokinase locus on chromosome 7p to early-onset non-insulin-dependent diabetes mellitus. Nature 356, 162-164

Gromada, J., Brock, B., Schmitz, O., and Rorsman, P. (2004). Glucagon-like peptide-1: regulation of insulin secretion and therapeutic potential. Basic. Clin. Pharmacol. Toxicol. *95*, 252-262.

Henquin, J. C., Ravier, M. A., Nenquin, M., Jonas, J. C., and Gilon, P. (2003). Hierarchy of the β-cell signals controlling insulin secretion. Eur. J. Clin. Invest. 33, 742-750.

Kahn, S.E. (2000). The importance of the beta-cell in the pathogenesis of type 2 diabetes mellitus. Am. J. Med. *108*, 2S-8S.

Lacy, P.E., and Kostianovsky, M. (1967). Method for the isolation of intact islets of Langerhans from the rat pancreas. Diabetes *16*, 35-39.

Lishko, P.V., Botchkina, I.L., Fedorenko, A., and Kirichok, Y. (2010). Acid extrusion from human spermatozoa is mediated by flagellar voltage-gated proton channel. Cell *140*, 327-337.

Martin, B.C., Warram, J.H., Krolewski, A.S., Bergman, R.N., Soeld-ner, J.S., and Kahn, C.R. (1992). Role of glucose and insulin resis- tance in development of type II diabetes mellitus: results of a 25- year follow-up study. Lancet *340*, 925-929.

Matschinsky, F.M., Glaser, B., and Magnuson, M.A. (1998). Pancreatic beta-cell glucokinase: closing the gap between theoretical concepts and experimental realities. Diabetes *47*, 307-315.

McQuaid, T.S., Saleh, M.C., Joseph, J.W. Gyulkhandanyan, A., Manning-Fox, J.E., MacLellan, J.D., Wheeler, M.B., and Chan, C.B. (2006). cAMP-mediated signaling normalizes glucose-stimulated insulin secretion in uncoupling protein-2 overexpressing β-cells. J. Endocrinol. *190*, 669-680.

Nesher, R., Della Casa, L., Litvin, Y., Sinai, J., Del Rio, G., Pevsner, B., Wax, Y., and Cerasi, E. (1987). Insulin deficiency and insulin resistance in type 2 (non-insulin-dependent) diabetes: quantitative contributions of pancreatic and peripheral responses to glucose homeostasis. Eur. J. Clin. Invest. *17*, 266-274.

Okochi, Y., Sasaki, M., Iwasaki, H., and Okamura, Y. (2009). Voltage-gated proton channel is expressed on phagosomes. Biochem. Biophys. Res. Commun. *382*, 274-279.

Olefsky, J.M., and Glass, C.K. (2010). Macrophages, inflammation, and insulin resistance. Annu. Rev. Physiol. *72*, 219-246.

Pfeifer, M.A, Halter, J.B, Beard, J.C, Judzewitsch, R, and Porte, D Jr. (1982). Insulin responses to nonglucose stimuli in non-insulin-dependent diabetes mellitus during a tolbutamide infusion. Diabetes 31, 154-159.

Poitout, V., and Robertson, R.P. (1996). An integrated view of beta-cell dysfunction in type II diabetes. Annu. Rev. Med. *47*, 69-83.

Polonsky, K.S. (1995). Lilly Lecture 1994. The beta-cell in diabetes: from molecular genetics to clinical research. Diabetes *44*, 705-717.

Porte, D., Jr. (1991). Banting lecture 1990. Beta-cells in type II diabetes mellitus. Diabetes *40*, 166–180.

Prentki, M., and Matschinsky, F.M. (1987). Ca^{2+}, cAMP, and phospholipid-derived messengers in coupling mechanisms of insulin secretion. Physiol. Rev. 67, 1185-1248.

Proks, P., Reimann, F., Green, N., Gribble, F., Ashcroft, F. (2002). Sulfonylurea stimulation of insulin secretion. Diabetes *51* (Suppl 3), S368-376.

Rahier, J., Guiot, Y., Goebbels, R.M., Sempoux, C., and Henquin, J.C. (2008). Pancreatic beta-cell mass in European subjects with type 2 diabetes. Diabetes Obes. Metab. *10* (Suppl 4), 32-42.

Ramsey, I.S., Moran, M.M., Chong, J.A., and Clapham, D.E. (2006). A voltage-gated proton-selective channel lacking the pore domain. Nature *440*, 1213-1216.

Ramsey, I.S., Ruchti, E., Kaczmarek, J., and Clapham, D.E. (2009). Hv1 proton channels are required for high-level NADPH oxidase-dependent superoxide production during the phagocyte respiratory burst. Proc. Natl. Acad. Sci. U.S.A. *106*, 7642-7647.

Rorsman, P., and Renstrom, E. (2003). Insulin granule dynamics in pancreatic beta cells. Diabetologia *46*, 1029-1045.

Seino, S., Takahashi, H., Fujimoto, W., and Shibasaki1, T. (2009). Roles of cAMP signalling in insulin granule exocytosis. Diabetes Obes. Metab. *11*, 180-188.

Temple, R.C., Carrington, C.A., Luzio, S.D., Owens, D.R., Schneider, A.E., Sobey, W.J., and Hales, C.N. (1989). Insulin deficiency in non-insulin-dependent diabetes. Lancet *1*, 293-295.

Unger, R.H. (1991). Diabetic hyperglycemia: link to impaired glucose transport in pancreatic β cells. Science *251*, 1200-1205.

Wang, Y., Li, S.J., Pan, J., Che, Y., Yin, J., and Zhao, Q. (2011). Specific expression of the

human voltage-gated proton channel Hv1 in highly metastatic breast cancer cells, promotes tumor progression and metastasis. Biochem. Biophys. Res. Commun. *412*, 353-359

Wang, Y., Li, S.J., Wu, X., Che, Y., and Li, Q. (2012). Clinicopathological and Biological Significance of Human Voltage-gated Proton Channel Hv1 Protein Overexpression in Breast Cancer. J. Biol. Chem. *287*, 13877-13888.

Wang, Y., Wu, X., Li, Q., Zhang, S., and Li, S.J. (2013a). Human Voltage-Gated Proton Channel Hv1: A New Potential Biomarker for Diagnosis and Prognosis of Colorectal Cancer. PLoS One *8*, e70550.

Wang, Y., Zhang, S., and Li, S.J. (2013b). Zn^{2+} induces apoptosis in human highly metastatic SHG-44 glioma cells, through inhibiting activity of the voltage-gated proton channel Hv1. Biochem. Biophys. Res. Commun. *438*, 312-317

Warram, J.H., Rich, S.S. & Krolewski, A.S. Joslin's Diabetes Mellitus (eds Kahn, C.R. & Weir, G.C.) 201-215 (Philadelphia, Lea & Febiger, 1994).

Weinhaus, A.J., Poronnik, P., Tuch, B.E., and Cook, D.I. (1997). Mechanisms of arginine-induced increase in cytosolic calcium concentration in the beta-cell line NIT-1. Diabetologia *40*, 374-382.

Weir, G.C., and Bonner-Weir, S. (2004). Five stages of evolving beta-cell dysfunction during progression to diabetes. Diabetes *53* (Suppl 3), S16-S21.

Wu, L.J., Wu, G., Sharif, M.R.A., Baker, A., Jia, Y., Fahey, F.H., Luo, H.R., Feener, E.P., and Clapham, D.E. (2012). The voltage-gated proton channel Hv1 enhances brain damage from ischemic stroke. Nat. Neurosci.*15*, 565-573.

Zhao, Q., Che, Y., Li, Q., Zhang, S., Gao, Y.T., Wang, Y., Wang, X., Xi, W., Zuo, W., and Li, S.J. (2015). The voltage-gated proton channel Hv1 is expressed in pancreatic islet β-cells and regulates insulin secretion. Biochem. Biophys. Res. Commun. *468*, 746-751.

FIGURE LEGENDS

FIGURE 1. Hv1-deficient mice exhibit hyperglycaemia and impaired glucose tolerance with reduced insulin secretion.

A: Body weight change of KO, heterozygous and WT mice ($n^{+/+}$ = 24; $n^{+/-}$ = 24; $n^{-/-}$ = 24). Data are mean ± SEM.

B: Basal blood glucose concentrations after fasting 6 h in 4 month-old KO, heterozygous and WT mice ($n^{+/+}$ = 24; $n^{+/-}$ = 24; $n^{-/-}$ = 24). Data are mean ± SEM. ***P < 0.001, KO or heterozygous vs. WT.

C: Blood glucose levels measured in whole blood following i.p. injection of glucose (2 g/kg body weight) in KO, heterozygous and WT mice ($n^{+/+}$ = 12; $n^{+/-}$ = 12; $n^{-/-}$ = 12). Data are means ± SEM. *P < 0.05, ***P < 0.001, KO vs. WT.

D: Insulin concentrations measured in sera of KO, heterozygous and WT mice following i.p. glucose challenge (2 g/kg body weight) ($n^{+/+}$ = 8; $n^{+/-}$ = 8; $n^{-/-}$ = 8). Data are means ± SEM. *P < 0.05, ***P < 0.001, KO vs. WT. Hv1KO mice exhibit a loss of acute phase insulin secretion in response to glucose.

E: Insulin concentrations measured in sera of KO, heterozygous and WT mice following i.p. L-arginine challenge (1 g/kg body weight) ($n^{+/+}$ = 8; $n^{+/-}$ = 8; $n^{-/-}$ = 8). Data are means ± SEM. *P < 0.05, **P < 0.01, KO vs. WT. Hv1KO mice show a markedly decreased arginine-stimulated insulin secretion, but retaining first-phase secretion.

F: Blood glucose levels measured in whole blood following i.p. insulin injection (1 U/kg body weight) in KO, heterozygous and WT mice ($n^{+/+}$ = 12; $n^{+/-}$ = 12; $n^{-/-}$ = 12). Data are means ± SEM.

FIGURE 2. Hv1KO mice at 2 months of age exhibit an progressively impaired glucose tolerance with age due to significantly reduced insulin secretion.

A: Blood glucose levels measured in whole blood following i.p. injection of glucose (2 g/kg body weight) in KO and WT mice ($n^{+/+}$ = 10; $n^{-/-}$ = 10). Data are means ± SEM. *P < 0.05, KO vs. WT.

B: Insulin concentrations measured in sera of KO and WT mice following i.p. glucose

challenge (2 g/kg body weight) ($n^{+/+}$ = 8; $n^{-/-}$ = 8). Data are means ± SEM. ***P* < 0.01, ****P* < 0.001, KO vs. WT. Hv1KO mice exhibit a significant loss of phase insulin secretion in response to glucose.

C: Insulin concentrations measured in sera of KO and WT mice following i.p. L-arginine challenge (1 g/kg body weight) ($n^{+/+}$ = 8; $n^{-/-}$ = 8). Data are means ± SEM. ***P* < 0.01, ****P* < 0.001, KO vs. WT. Hv1KO mice show a markedly decrease to respond to a arginine stimulus, but retaining its response to arginine.

F: Blood glucose levels measured in whole blood following i.p. insulin injection (1 U/kg body weight) in KO and WT mice ($n^{+/+}$ = 10; $n^{-/-}$ = 10). Data are means ± SEM.

FIGURE 3. Reduced insulin secretion of islets from Hv1-deficient mice.

A: Glucose-, sulfonylurea-, KCl- and L-arginine-induced insulin secretion from isolated islets of KO, heterozygous and WT mice (n = 8 per genotype). Data are means ± SEM. ****P* < 0.001, heterozygous vs. corresponding WT; $^{\#\#\#}P$ < 0.001, KO vs. corresponding WT; $^{\&\&\&}P$ < 0.001, Glc, Tol, Glb, KCl or Arg vs. Basal for WT. Basal, 2.8 mM glucose; Glc, 16.7 mM glucose; Tol, 200 μM tolbutamide; Glb, 1 μM glibenclamide; KCl, 60 mM KCl; Arg, 10 mM L-arginine.

B and C: Insulin (B) and proinsulin (C) contents at a basal condition (2.8 mM glucose) in isolated islets from KO , heterozygous and WT mice (n = 8 per genotype). Data are means ± SEM. ***P* < 0.01, ****P* < 0.001, KO vs. corresponding WT.

D: Ratio of insulin to proinsulin content of isolated islets of KO, heterozygous and WT mice at a basal condition (n = 8 per genotype). Data are means ± SEM. NS (no significance), vs. WT.

E: Proinsulin secretion at 16.7 mM glucose from isolated islets of KO, heterozygous and WT mice (n = 8 per genotype). Data are mean ± SEM. ****P* < 0.001, KO or heterozygous vs. WT.

F: Ratio of insulin to proinsulin secretion of isolated islets of KO, heterozygous and WT mice at 16.7 mM glucose (n = 8 per genotype). Data are means ± SEM. NS (no significance), vs. WT.

FIGURE 4. siRNA-mediated knockdown of Hv1 inhibits secretagogue-induced insulin secretion.

A: Glucose- and sulfonylurea-induced insulin secretion from INS-1 (832/13) β cells transfected with scramble (control) or Hv1-targeting siRNA (siRNA) (n = 8 per condition). Data are mean ± SEM. $^{**}P < 0.01$,$^{***}P < 0.001$, vs. corresponding control; $^{\#\#\#}P < 0.01$, vs. control at basal.

B and C: Insulin (B) and proinsulin (C) contents in the β cells transfected with scramble (control) or Hv1-targeting siRNA (siRNA) at a basal condition (n = 8 per condition). Data are mean ± SEM. $^{***}P < 0.001$, vs. corresponding control.

D: The ratio of insulin to proinsulin content of the β cells transfected with scramble (control) or Hv1-targeting siRNA (siRNA) at a basal condition (n = 8 per condition). Data are mean ± SEM. NS (no significance), vs. control.

E and F: Quantitative RT-PCR for insulin from INS-1 (832/13) β cells (E) and isolated islets (F) treated with scramble (control) or Hv1-targeting siRNA (siRNA). Data are mean ± SEM (n = 3 per condition). $^{*}P < 0.05$, vs. corresponding control.

G and H: Proinsulin secretion (G) and the ratio of insulin to proinsulin secretion (H) of INS-1 (832/13) β cells transfected with scramble (control) or Hv1-targeting siRNA (siRNA) in the presence of 16.7 mM glucose. Data are mean ± SEM (n = 8 per condition). $^{**}P < 0.01$, $^{***}P < 0.001$, NS (no significance), vs. corresponding control. These data suggests that no significant accumulation of proinsulin occurred in KO islets.

FIGURE 5. Knockout of Hv1 decreases α and β cell masses.

A: Immunohistochemical analysis of 4 month-old WT, heterozygous and KO islets using anti-insulin and anti-glucagon antibodies. Representative images of H&E, anti-insulin and anti-glucagon antibody-stained pancreatic sections from 4 month-old WT, heterozygous and KO mice. Scale bar, 50 μm.

B: Relative islet area of 4 month-old WT and KO mice analyzed by immunohistochemistry of pancreatic sections (n = 6 per genotype). Data are mean ± SEM. $^{*}p < 0.05$, vs. WT.

C and D: α and β cell masses of 4 month-old WT and KO mice based on immunostaining of pancreatic sections (n = 6 per genotype). Relative α and β cell masses were determined as a ratio of total glucagon (α cell)- or insulin (β cell)-positive area to total pancreatic area. Twenty to thirty sections per pancreas were analyzed. Data are presented as mean ± SEM. $*p < 0.05$, $**p < 0.01$, vs. corresponding WT.

E: Pancreatic insulin content (n = 6 per genotype). Data are mean ± SEM. $*p < 0.05$, vs. WT.

FIGURE 6. Deficiency of Hv1 has no effect on cAMP generation in β cells, but impairs cellular Ca^{2+} homeostasis and membrane depolarization.

A: Insulin secretion of isolated islets transfected with scramble (control) or Hv1-targeting siRNA (siRNA) at 2.8 mM glucose, 2.8 mM glucose containing 10 μM forskolin, and 16.7 mM glucose containing 10 μM forskolin (n = 8 per condition). Data are mean ± SEM. $*P < 0.05$, $**P < 0.01$, $***P < 0.001$, vs. corresponding control; $^{\#\#}P < 0.01$, $^{\#\#\#}P < 0.001$, vs. control at 2.8 mM glucose.

B: cAMP content of isolated islets transfected with scramble (control) or Hv1-targeting siRNA (siRNA) at 16.7 mM glucose containing 10 μM forskolin (n = 6 per condition). Data are mean ± SEM. NS (no significance), vs. control.

C: Insulin secretion of INS-1 (832/13) β cells transfected with scramble (control) or Hv1-targeting siRNA (siRNA) at 16.7 mM glucose and in the presence of 10 or 100 nM GLP-1 (n = 6 per condition). Data are mean ± SEM. $***P < 0.001$, vs. corresponding control; $^{\#\#\#}P < 0.001$, vs. control without GLP-1.

D, E and F: Knockdown of Hv1 impairs cellular Ca^{2+} homeostasis in β cells. Cellular Ca^{2+} levels in INS-1 (832/13) β cells were measured by Fura-2 fluorescence. The β cells treated with scramble siRNA (control) or Hv1-targeting siRNA (siRNA) were kept at 2.8 mM glucose before switching to stimulation by 200 μM tolbutamide without (D) or with (E) 16.7 mM glucose as indicated above the traces. The β cells were kept at 2.8 mM glucose before switching to stimulation by 200 μM tolbutamide without or with 10 μM $ZnCl_2$ as indicated above the traces (F). This result indicates that Zn^{2+}, a classical inhibitor of Hv1

(24, 25) (Ramsey et al., 2006; DeCoursey, 2008), can efficiently inhibit Ca^{2+} influx in the β cell.

G and H. Knockdown of Hv1 impairs membrane depolarization induced by glucose or tolbutamide in β cells. The membrane potential changes of INS-1 (832/13) β cells during glucose- and tolbutamide-stimulation were monitored by $DiBAC_4(3)$ fluorescence. INS-1 (832/13) β cells treated with scramble siRNA (control) or Hv1-targeting siRNA (siRNA) were kept at 2.8 mM glucose before switching to stimulation by 16.7 mM glucose (G) or 200 μM tolbutamide (H) as indicated above the traces.

Fig. 1

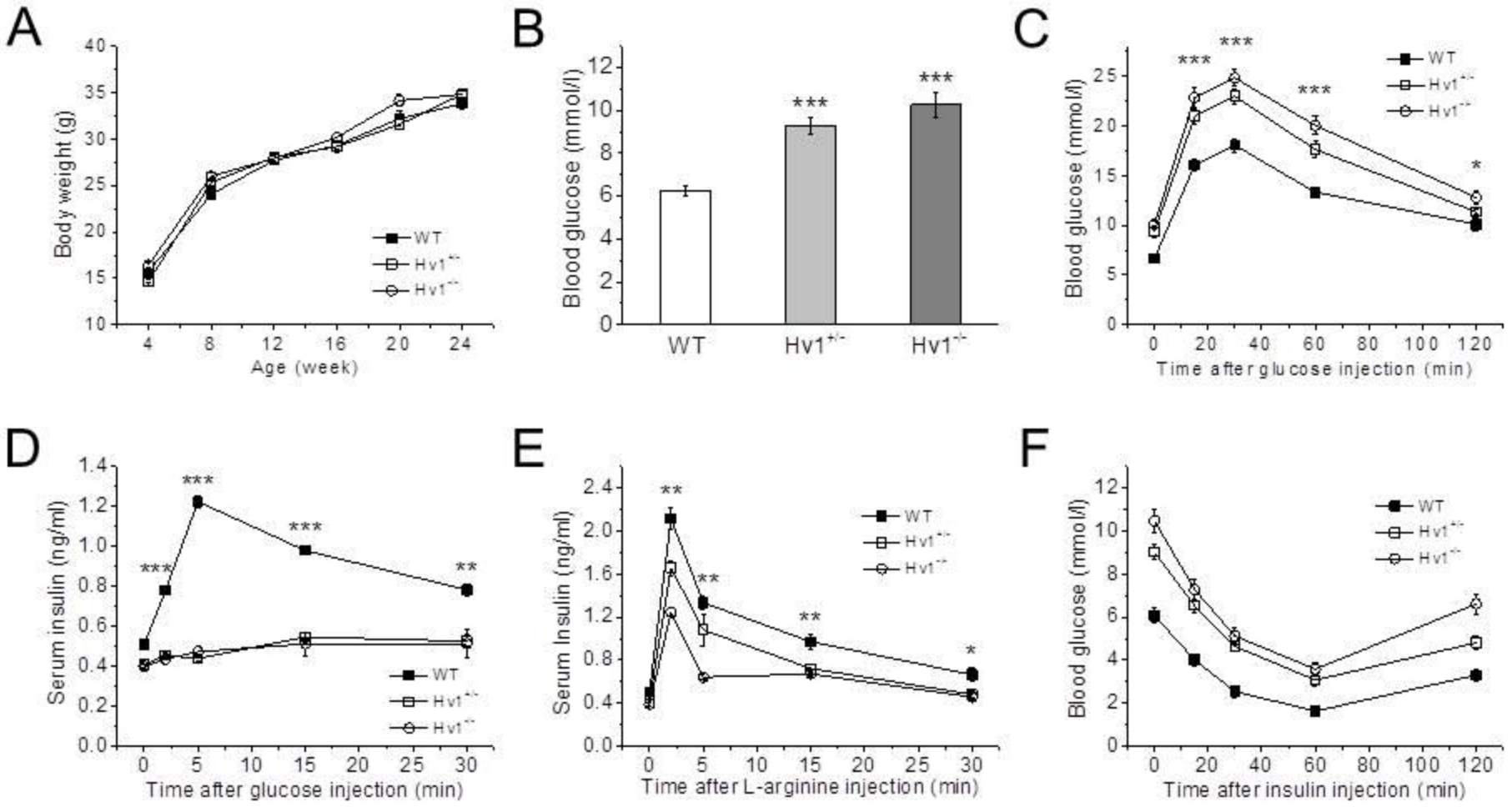
A
Body weight (g)
Age (week)
WT
Hv1+/-
Hv1-/-
B
Blood glucose (mmol/l)
WT
Hv1+/-
Hv1-/-
***
C
Blood glucose (mmol/l)
Time after glucose injection (min)
WT
Hv1+/-
Hv1-/-
***
*
D
Serum insulin (ng/ml)
Time after glucose injection (min)
WT
Hv1+/-
Hv1-/-
***
**
E
Serum Insulin (ng/ml)
Time after L-arginine injection (min)
WT
Hv1+/-
Hv1-/-
**
*
F
Blood glucose (mmol/l)
Time after insulin injection (min)
WT
Hv1+/-
Hv1-/-

Fig. 2

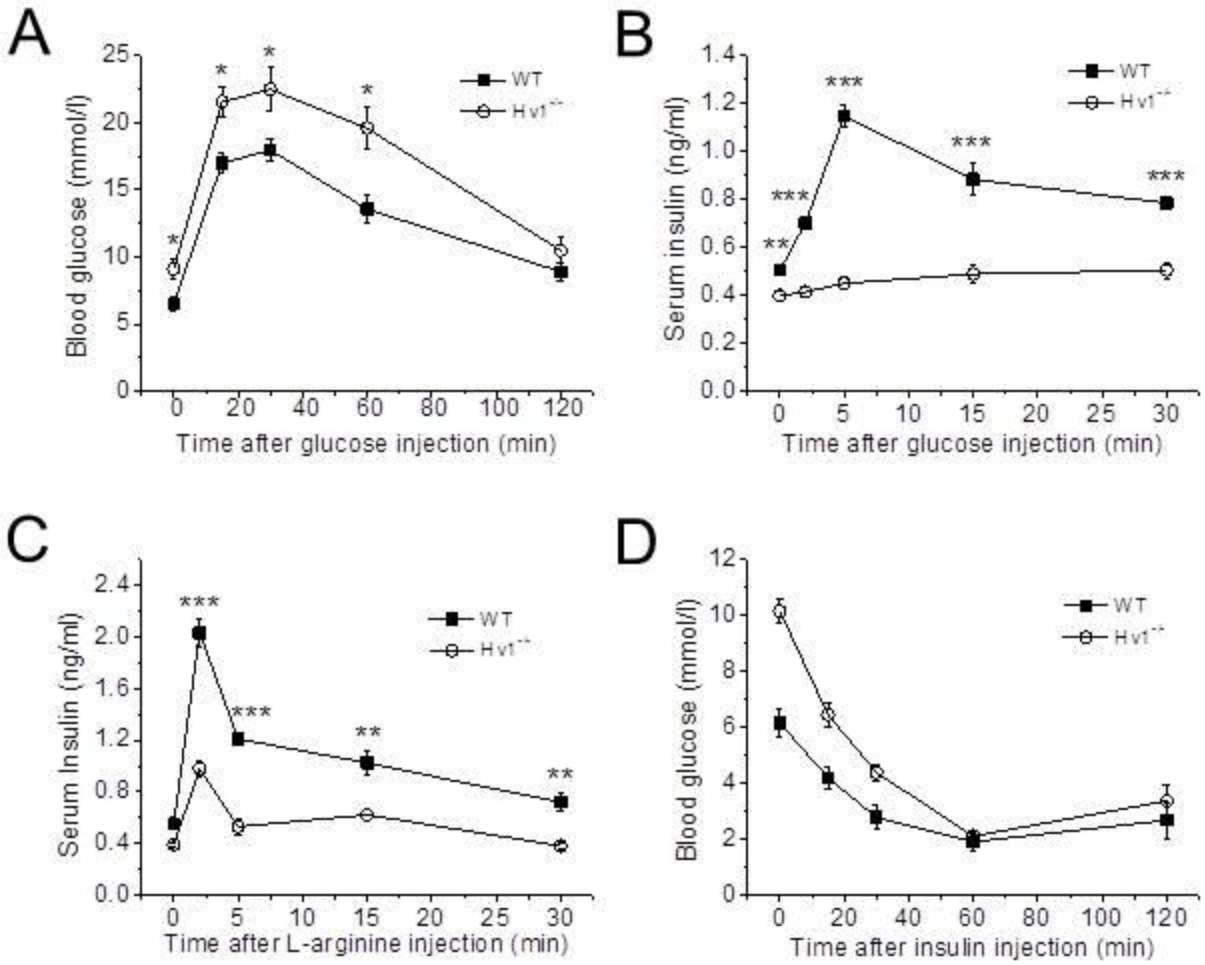
A
Blood glucose (mmol/l)
Time after glucose injection (min)
WT
Hv1-/-
B
Serum insulin (ng/ml)
Time after glucose injection (min)
C
Serum Insulin (ng/ml)
Time after L-arginine injection (min)
D
Blood glucose (mmol/l)
Time after insulin injection (min)

Fig. 3

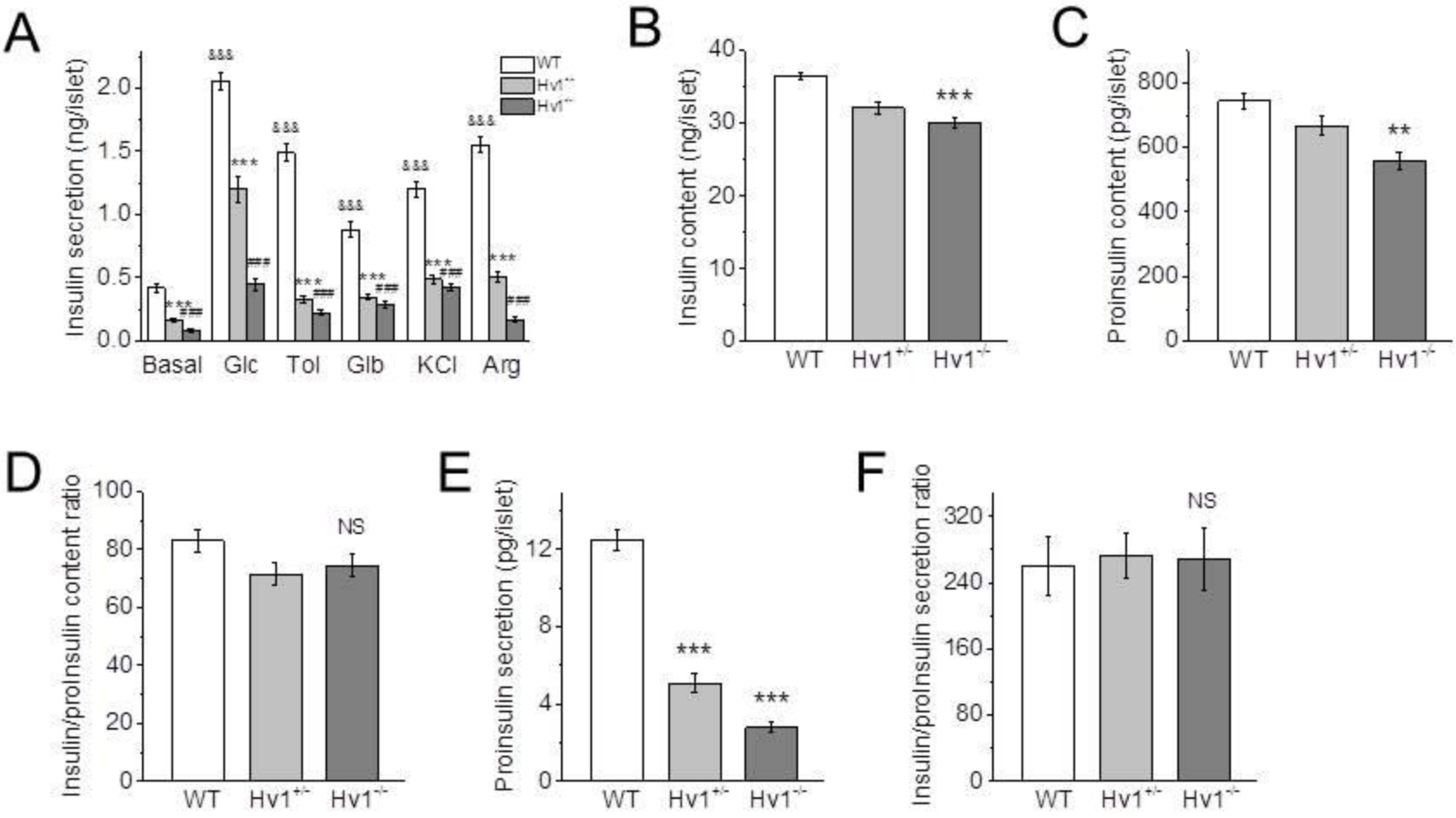
A
Insulin secretion (ng/islet)
2.0
1.5
1.0
0.5
0.0
WT
Hv1+/-
Hv1-/-
&&&
***
###
Basal
Glc
Tol
Glb
KCl
Arg
B
Insulin content (ng/islet)
40
30
20
10
0
***
WT
Hv1+/-
Hv1-/-
C
Proinsulin content (pg/islet)
800
600
400
200
0
**
WT
Hv1+/-
Hv1-/-
D
Insulin/proInsulin content ratio
100
80
60
40
20
0
NS
WT
Hv1+/-
Hv1-/-
E
Proinsulin secretion (pg/islet)
12
8
4
0
***
***
WT
Hv1+/-
Hv1-/-
F
Insulin/proInsulin secretion ratio
320
240
160
80
0
NS
WT
Hv1+/-
Hv1-/-

Fig. 4

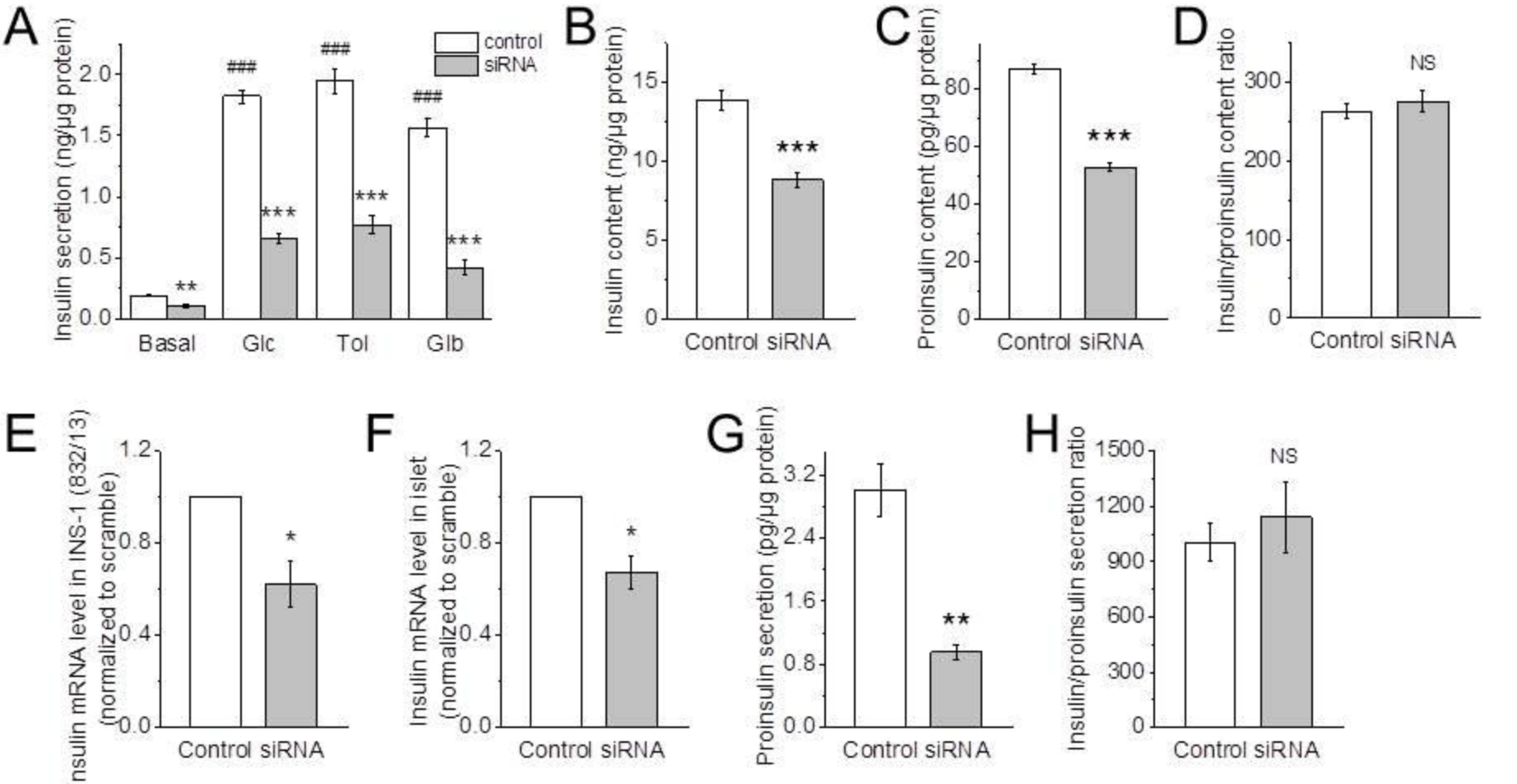
A
Insulin secretion (ng/μg protein)
control
siRNA
###
**
***
Basal
Glc
Tol
Glb
B
Insulin content (ng/μg protein)
Control siRNA
C
Proinsulin content (pg/μg protein)
Control siRNA
D
Insulin/proinsulin content ratio
NS
Control siRNA
E
Insulin mRNA level in INS-1 (832/13) (normalized to scramble)
Control siRNA
F
Insulin mRNA level in islet (normalized to scramble)
Control siRNA
G
Proinsulin secretion (pg/μg protein)
Control siRNA
H
Insulin/proinsulin secretion ratio
NS
Control siRNA

Fig. 5

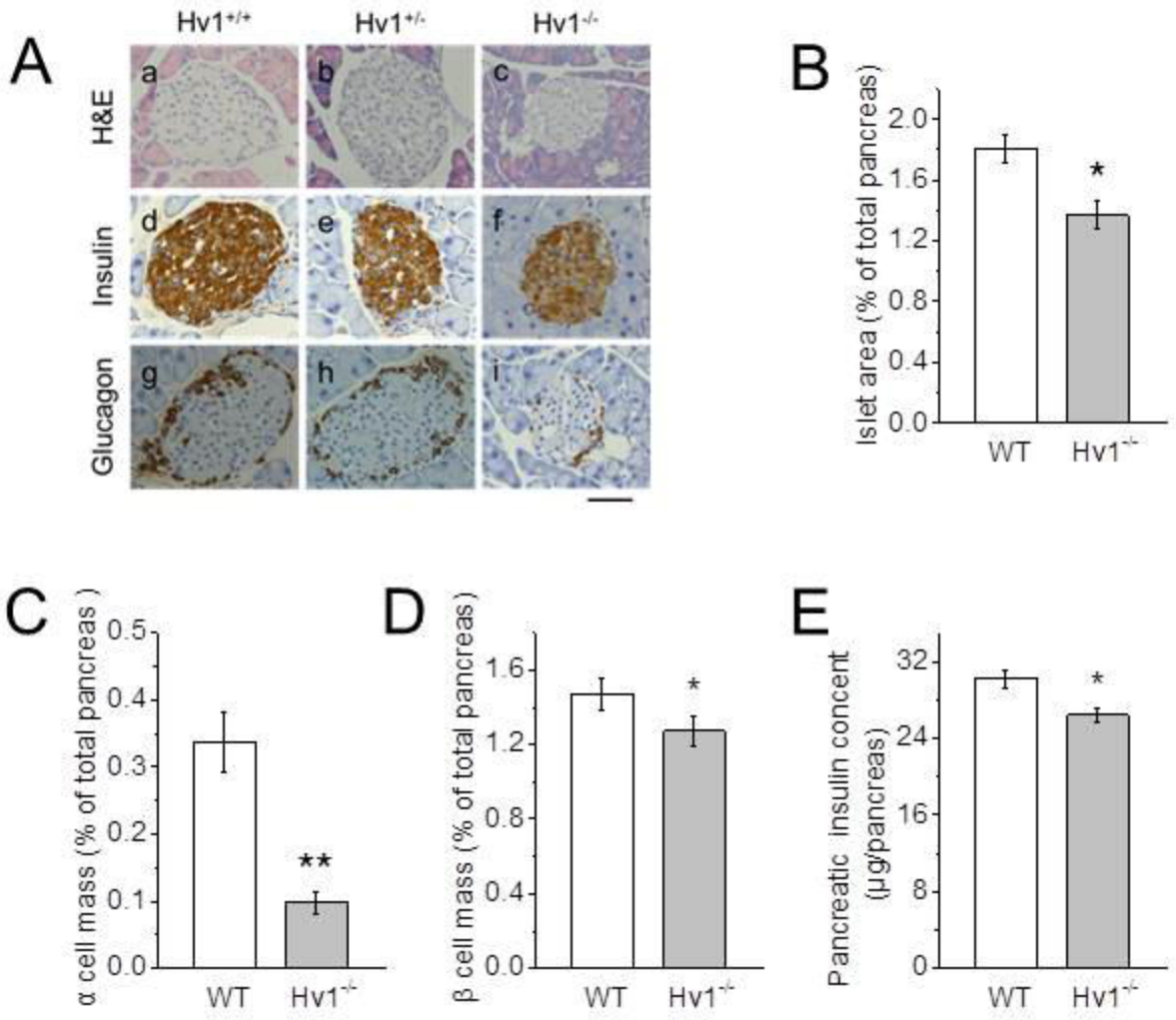
A
Hv1+/+
Hv1+/-
Hv1-/-
H&E
Insulin
Glucagon
a
b
c
d
e
f
g
h
i
B
Islet area (% of total pancreas)
2.0
1.6
1.2
0.8
0.4
0.0
*
WT
Hv1-/-
C
α cell mass (% of total pancreas)
0.5
0.4
0.3
0.2
0.1
0.0
**
WT
Hv1-/-
D
β cell mass (% of total pancreas)
1.6
1.2
0.8
0.4
0.0
*
WT
Hv1-/-
E
Pancreatic insulin concent (μg/pancreas)
32
24
16
8
0
*
WT
Hv1-/-

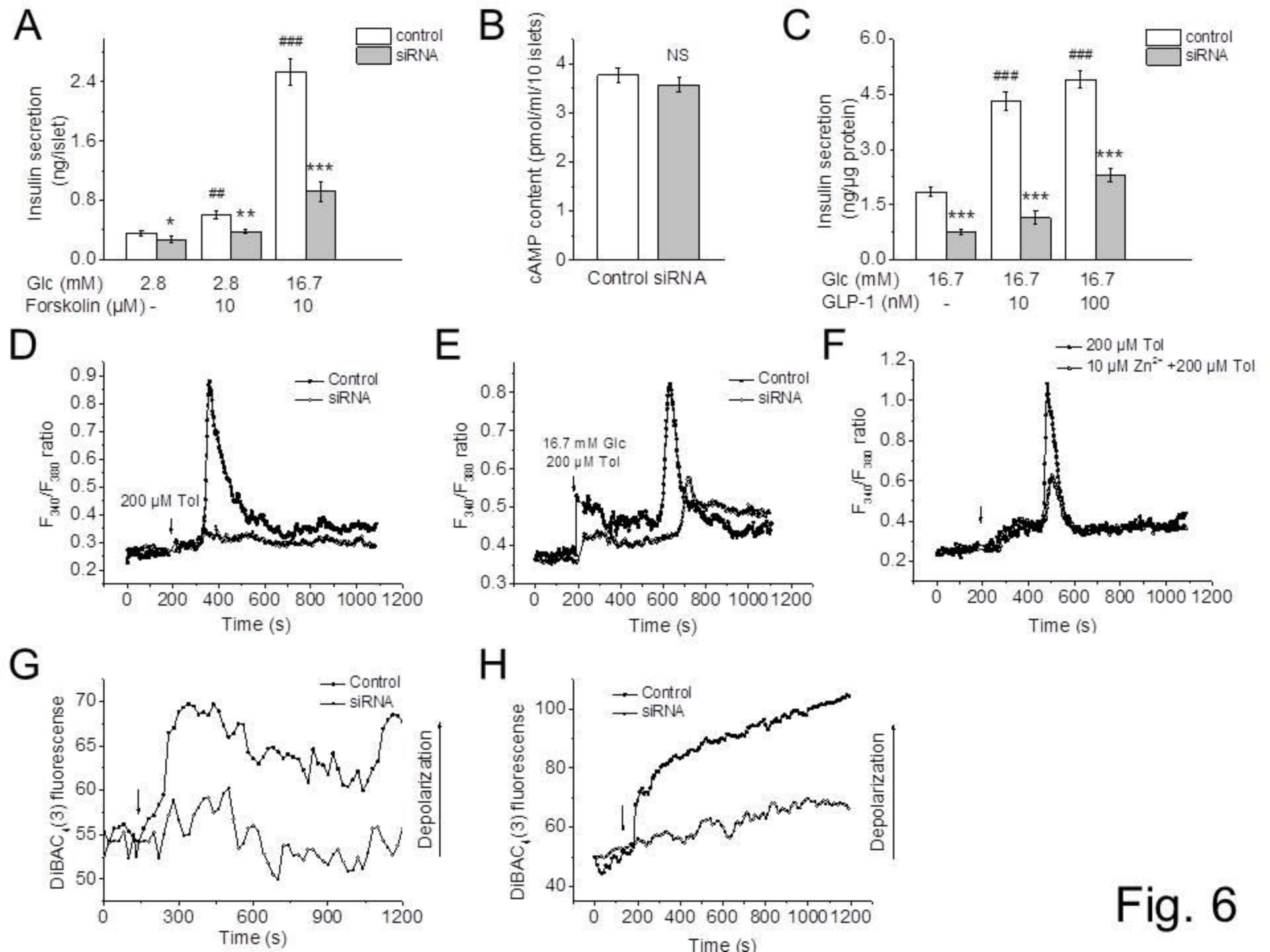
A
control
siRNA
Insulin secretion (ng/islet)
0.0
0.8
1.6
2.4
*
##
**
###
***
Glc (mM) 2.8 2.8 16.7
Forskolin (μM) - 10 10
B
cAMP content (pmol/ml/10 islets)
0
1
2
3
4
NS
Control siRNA
C
control
siRNA
Insulin secretion (ng/μg protein)
0.0
1.5
3.0
4.5
6.0
***
###
***
###
***
Glc (mM) 16.7 16.7 16.7
GLP-1 (nM) - 10 100
D
Control
siRNA
F_{340}/F_{380} ratio
200 μM Tol
Time (s)
E
Control
siRNA
16.7 mM Glc
200 μM Tol
F_{340}/F_{380} ratio
Time (s)
F
200 μM Tol
10 μM Zn^{2+} +200 μM Tol
F_{340}/F_{380} ratio
Time (s)
G
Control
siRNA
$DiBAC_4(3)$ fluorescense
Depolarization
Time (s)
H
Control
siRNA
$DiBAC_4(3)$ fluorescense
Depolarization
Time (s)

Fig. 6